Hybrid Aerial-Aquatic Vehicle for Large Scale High Spatial Resolution Marine Observation

Jiayi Wang&
State Key Laboratory of Ocean Engineering
Institute of Electronic Information and Electrical Engineering
Shanghai Jiao Tong University
Shanghai, China
1257191427@sjtu.edu.cn

Yiwei Yang&
State Key Laboratory of Ocean Engineering
University of Michigan-Shanghai Jiao Tong University Joint Institute
Shanghai Jiao Tong University
Shanghai, China
yyw0063@sjtu.edu.cn

Jiajin Wu&
State Key Laboratory of Ocean Engineering
University of Michigan-Shanghai Jiao Tong University Joint Institute
Shanghai Jiao Tong University
Shanghai, China
awbjcj@sjtu.edu.cn

Zheng Zeng
State Key Laboratory of Ocean Engineering
School of Oceanography
Shanghai Jiao Tong University
Shanghai, China
zheng.zeng@sjtu.edu.cn

Di Lu
State Key Laboratory of Ocean Engineering
School of Oceanography
Shanghai Jiao Tong University
Shanghai, China
lltom@sjtu.edu.cn

Lian Lian
State Key Laboratory of Ocean Engineering
School of Oceanography
Shanghai Jiao Tong University
Shanghai, China
llian@sjtu.edu.cn

&: These authors contributed equally to this work and should be considered co-first authors

***Abstract*—Hybrid Aerial-Aquatic Vehicle (HAAV), which is a hybrid of underwater gliders and fixed-wing drone, is energy-efficient, highly maneuverable and suitable for marine observation of large scale and high spatial resolution. In this paper, a novel scheme is proposed for autonomously sampling multiple water columns in relative short time with long distance and complex obstacles between each other using (HAAV). The scheme exploits energy-efficient spiral-down motion to sample each water column, followed by the pull-up motion with the propeller into the sky and fly to the next water column. Once flying, the vehicle uses both Global Positioning System guidance and Remote-controlled System to reach the next column location. To enhance the path-tracking performance, closed-loop control is used in the spiral motion, and a depth transducer is installed to regulate depth during gliding. The HAAV prototype has undergone the field test in both Shanghai Jiao Tong University Underwater Engineering Institute Co. (SJTU-UEIC) and Zhiyuan Lake at depths of 1, 2 and 0.5 meter. MATLAB Simulink together with the time-stamped photos are also used to simulate the gestures during the process of egression and gliding with the data recorded by the sensors so that detailed improvement can be achieved in the future.**

Keywords—hybrid vehicle, water column sampling, glider, marine observation

I. Introduction

Monitoring and understanding aquatic environments is an ongoing challenge. To know the ocean layers and currents better, it is essential to measure the physical water parameters in large-scale high-spatial resolution. But up to now, the feasible ways of measurement has remained to be a critical bottleneck to the marine observation.

Water column sampling is one of the ways to evaluate the stratification of water layers at various depths of water, which can analyze the variation of mixtures at a specific area of the water along the depth direction [1]. Large spatial scale and high resolution are desired during water column sampling [2]. Sometimes multiple water columns need to be evaluated in a water area. The objective of the Hybrid Aerial-Aquatic Vehicle (HAV) is to measure the physical water parameters in large-scale high-spatial resolution based on the method of water column sampling.

Traditional observing methodologies relied on manned vessels or fixed monitoring buoys are far from meeting the desired spatial and temporal resolution. In recent years, people have focused on developing marine robotics specialized in aquatic environment operation.

There are many kinds of autonomous vehicles for marine observation, including underwater gliding robotic fish, combined small-sized USV-ROV observation system, morphing aquatic Micro Aerial Vehicle (MAV), hybrid aerial underwater vehicle, etc.

Most of these autonomous vehicles are brand new concepts and have their own advantages. However, despite the novel design, most of them are not suitable for large scale and high spatial resolution marine observation, in other words, operating in large open-water areas and sampling at deep or distant places for long duration with high resolution.

Underwater gliding robotic fish is energy-efficient and highly-maneuverable, it moves even slower than USV-ROV system and since it can only stay underwater, bad weather or marine conditions like storm or turbulence may destroy it easily [1] [2]. Although the combined small-sized USV-ROV observation system acquires longer duration, it is also spatially-limited and therefore not suitable for large open-water areas because either ROV or USV moves slowly compared to any kind of UAVs [3] [4]. Morphing aquatic MAV uses a water jet thruster to take off and propel, meaning that although it moves fast, its duration time is extremely short. The spatially available area is also limited because it has to be launched from a USV base and requires additional

978-1-7281-1450-7/19/$31.00 ©2019 IEEE

efforts to deployed and recycled [5]. Hybrid aerial underwater vehicle looks like a quadcopter, and its four propellers enable it to move extremely fast. However, the propellers are so energy-consuming that the batteries cannot afford long distance or duration of sampling [6] [7] [8].

Therefore, almost all of these newly-designed vehicles have some disadvantages such as slow movement, energy-consuming, spatially restricted to certain location or difficult to deploy [9] [10]. No current technique displays the ability to sample quickly at multiple locations and bypass artificial and natural barriers like dams or icebergs. The goal is to combine the advantages and overcome the disadvantages mentioned above: fasten the speed of deployment and measurement at multiple locations, improve the spatial resolution and save the energy as much as possible for longer cruise.

We develop a hybrid aerial aquatic vehicle to improve the capability of data collection in the water column. The design intends to merge the benefits of operating in both aerial and underwater environments by combining the different configuration of either underwater glider or fixed-wing drone.

The invention is designed to fly as a fixed-wing drone between several target locations specified by scientists for the measurement of water column. Wings with large wingspan could provide enough elevating force to ensure long endurance. Since the vehicle can fly between the target locations, it is able to surmount artificial or natural obstacles like dams, bridges, or icebergs. In that case, lots of time and effort can be saved to deploy and recycle the vehicle.

When the vehicle is collecting data in the water column, it dives as an underwater glider, a kind of vehicle that glides in the water by adjusting its center of buoyancy and gravity to travel further with less energy consumption. Meanwhile, vertical and horizontal tails are also installed to achieve higher mobility. Thanks to the tail wing, the spiral motion of the vehicle can be restricted to a vertical cylinder whose diameter is less than one meter, meaning that the sampling and measurement of water column are of relatively high resolution. The schematic of the operation of the vehicle is shown in Fig. 1.

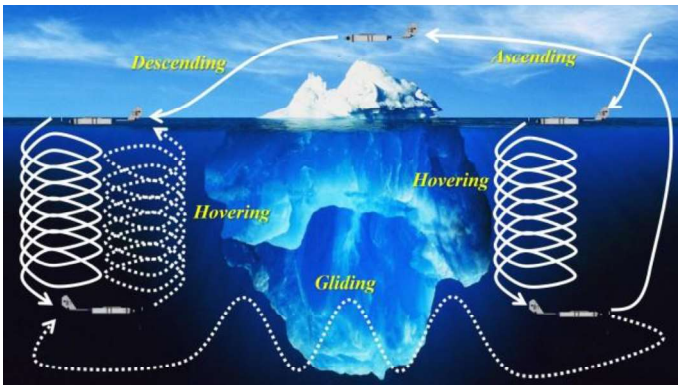

Fig. 1. Schematic of the operation of the vehicle.

This paper will present the sample operation scheme of the vehicle in Section II. Section III will cover the detailed explanation of various of systems of the vehicle, including the mechanical design, electrical design, etc. In Section IV, results of the field experiment, the performance in both aerial and underwater conditions will be provided.

II. Multi-Location Water Column Sampling Schemes

The vehicle is assigned a multi-position water sampling scheme. Scientists in the ground control station specify the target locations remains to be detected. The vehicle will receive the command and travel to these areas with either aerial or underwater method depending on the location the targets and surrounding terrain conditions. The data-collecting process is close-loop controlled. The vehicle controls its altitude according the feedback of water depth from its sensors and reaches the assigned depth in spiral motion. Meanwhile, it collects the parameters of the water column like location and temperature with other sensors aboard. After reaching the maximum depth allowed, the vehicle will fly or glide to the next target according to the command received from the scientists in the ground control station. The underwater gliding is preferred if the target location is not too far away and relatively easy to access to save the energy. Flying mode will be selected in case there is long distance between targets or the terrain condition around the location is complex.

The vehicle is featured with two operation mode: auto and manual. In auto-control mode, scientists only need to set the GPS coordinates of the locations, the related topographic map and the maximum depth allowed, then the vehicle will select the best routine and method to reach each place and do measurements. Manual-operated mode is designed mainly for emergency and maintenance. In this mode, operators can control the vertical and horizonal tails and the buoyancy system freely.

III. Mechanical Design & Assembling And Electronics & Control Systems Of The Vehicle

In this part, the vehicle will be decomposed into four parts: the airframe, the buoyancy management system, the electronics system and the propulsion system. In this section, both mechanical and electrical components of each part will be presented in detail. The following paragraphs will discuss the four parts in sequence. The general schematic is shown in Fig. 2.

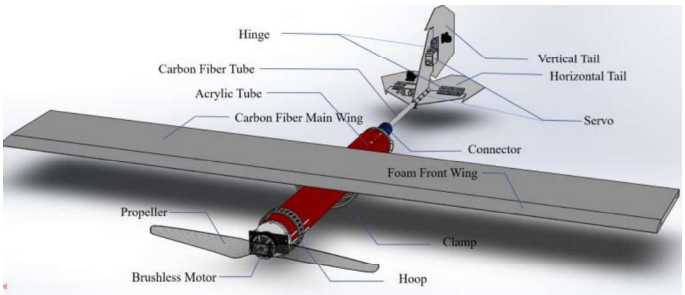

Fig. 2. The conceptual CAD design of the vehicle.

A. Airframe

The airframe is composed of four parts: the head, the body, the wing and the tail. The head consists of a brushless motor and its bracket, which will be introduced in detail in Part D, the propulsion system.

The wing is 870 mm in width, and is composed of two parts: the front wing and the main wing. The front wing is made up from foam to ensure that when the vehicle is diving underwater, buoyancy force is big enough to hold up the whole vehicle. Moreover, the front wing is streamline-shaped so that it is easier for the vehicle to take off when it is gliding on the surface of water. The main wing is composed of two pieces of carbon-fiber boards. Carbon-fiber wing is extremely light and strong enough to endure the resistance force from wind and water.

The body part is made up from the hull and two waterproof cover plates at both ends. The cover plate is comprised of an aluminum flange and an acrylic plate screwed by bolts. The flange is of waterproof usage and there are elaborately designed holes on the acrylic plate for the exchange of water between the inside and outside of the hull and the signal and data between the internal Micro-control Units (MCU) and external servos and transducers. The hull is a transparent acrylic tube whose inner, outer diameter and length is 50, 60 and 600 mm separately.

The tail is composed of vertical and horizontal carbon-fiber wings, both of which consists fixed parts and moveable parts. The fixed parts are connected to the carbon-fiber tube, and the moveable parts are attached to the fixed one through hinges, so that they can move flexibly. Two servos drives the moveable parts of both vertical and horizontal wings in four degrees of freedom, each about sixty degrees to adjust the direction and gesture of vehicle.

The parts mentioned above are connected to each other organically and form the skeleton of the vehicle. The functioning of all the parts will be displayed in the flow diagram in Fig. 4. The detailed dimensions of each main part are shown in Table I.

TABLE I.

THE DIMENSION AND WEIGHT OF MAIN PARTS OF VEHICLE.

Part	Dimension (mm)	Weight (kg)
Head	$100 * 90 * 50$	0.6
Wing	$870 * 220 * 30$	0.4
Body	$\Phi 60 * 600$	1.2
Tail	$200 * 160 * 220$	0.6

B. Buoyancy System

The buoyancy system is composed of a water sump, a water pump, a depth sensor, a flowmeter and a solenoid valve. All the components except for the sensor are shown in Fig. 3.

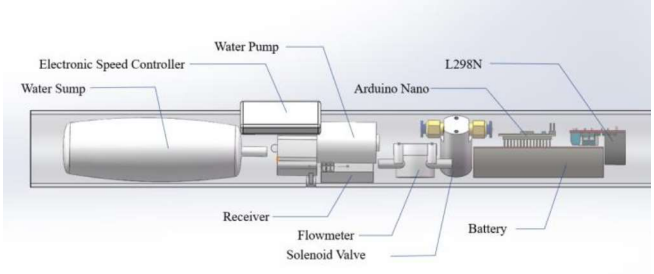

Fig. 3. Conceptual CAD design of the hull.

The water sump is a container to change the weight and center of mass to let the vehicle gliding underwater with its wings. It is connected to a water pump which is used to pump water and air into or out of the water sump through rubber tube. The pump is then connected to a flowmeter to record how much water has been pumped in or out. Then at the end of the rubber tube, there is a solenoid valve which is installed to resist the high pressure of water when the vehicle is diving underwater.

The depth sensor [Type: MS5837; Range: $0 - 30$ bar; Precision: 0.2 mbar (equivalent to 2 mm of the depth in water)] is fixed to the rear acrylic board and flange. Data of current pressure is collected by the sensor, converted to the depth and finally sent to the Arduino board for recording and close-loop control of the whole buoyancy system.

C. Electronic System

The hardware of electronic system is composed of a micro-control chip (Arduino Nano), a receiver, an electronic speed controller (ESC) and a voltage adaptor (L298N). The position of these hardware components can be found in Fig. 3.

L298N is a kind of voltage adaptor to provide enough voltage as well as the current to drive the water pump and solenoid valve. The maximum input voltage of L298N is 50 V. It is controlled with digital and analog signal transmitted by the Arduino Nano, a kind of micro-control chip (MCU). The receiver receives signal form a remote-control unit and controls the servos and waterproof electronic speed controller (ESC) which is attached to the outside surface of the hull for heat dissipation. Arduino Nano is powered by the receiver due to the relatively low voltage required for the micro-control chip to operate (less than 5 V). The battery provides power for L298N driver, the motor and the receiver. The flow diagram showing how each part operates and controls other parts is presented in Fig. 4.

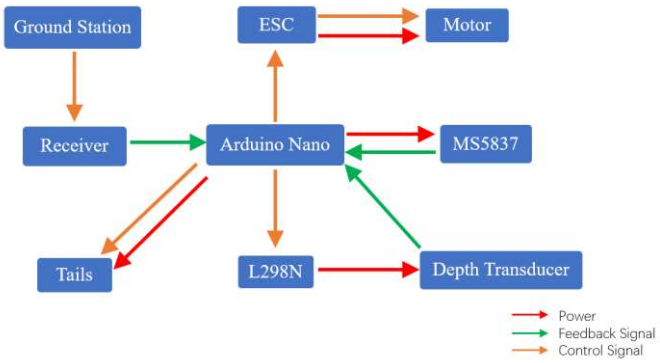

Fig. 4. The flow diagram of the vehicle.

D. The Propulsion System

The propulsion system is at the head of the whole vehicle. It is composed of a water-proof brushless motor whose rated voltage is 22.4 V and with the maximum thrust 4 kg. The foldable propeller is of 380 mm long when expanded and is installed on the tip of the brushless motor. The powerful motor and the propeller provide a force strong enough (more than 3.7 kg) to pull the vehicle up from the water into the sky. The total weight of the entire vehicle is only 2.8 kg according to Table 1, so that the 3.7 kg thrust is enough.

Since the motor require large current (about 10 A) to accelerate the motor for enough propulsion, a 22.4 V LiPo battery including six sub-batteries in parallel with the capacity of 1800 mAh in total is chosen. Each of the sub-batteries is featured with the discharge rate of 50 C. In that case, both the capacity and the current meet the demand of the vehicle to fly and dive for a relatively long period of time and distance. The anticipated performance of the vehicle is presented in Table II.

TABLE II.

THE ANTICIPATED PERFORMANCE OF THE VEHICLE.

Aerial Duration (min)	~20
Underwater Duration (min)	~60
Max Depth (m)	~10
Aerial Speed (m/s)	~10
Underwater Speed (m/s)	~0.3

IV. SIMULATION AND FIELD TEST OF THE VEHICLE

Due to limited conditions of the testing field in Shanghai Jiao Tong University Underwater Engineering Institute Co. (SJTU-UEIC), two operation modes--Egress & Gliding--were field tested to verify the vehicle's feasibility and maneuverability. Depth, vertical velocity and time were detected by sensors installed in the vehicle. Virtual simulations conducted by MATLAB Simulink covered the modelling of its horizontal velocity.

A. Egress

The egress process was modeled and analyzed with the assistant of Aerospace Blockset in MATLAB Simulink.

The aerodynamic coefficients of the vehicle were modeled by using DATCOM file. The overall coefficients of the vehicle--combining both aerodynamic and underwater coefficients--were approximated by interpolation. The initial depth was about 0.9m from the surface of water, which almost submerged the whole vehicle except for the propeller. The vehicle was initially pitching vertically up. The starting vertical velocity was set to be upwards to simulate the ending state of the underwater gliding operation.

Fig. 5.1 and Fig. 5.2 illustrates the relevant data during the egress operation. The vertical velocity grows smoothly. This is because the coefficients of the vehicle change gradually. The position of the horizontal tail remains unchanged during the whole process. Compared to the field test results which had significant drops in velocity, the simulation results are generally smooth since the coefficients are idealized and the tails remain fixed.

The pitching angle decreases while the yawing and rolling angles increases. This result is coincided with that of the field tests. However, the yawing and rolling angles change smaller than that during the field test. This is because the real vehicle might have its weight unbalanced. Additionally, the position of the tails might affect the egress trajectory.

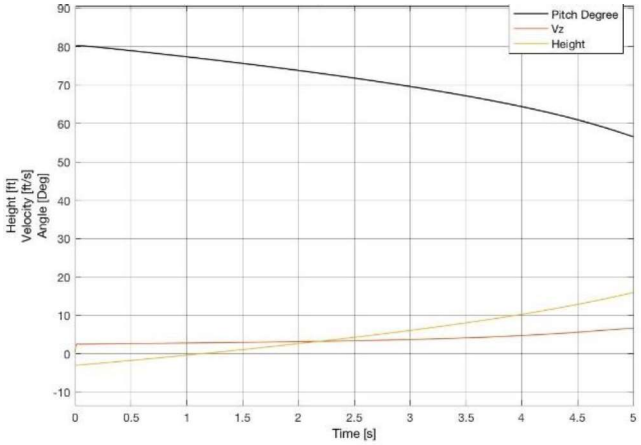

Fig. 5.1 Performance of egress (1).

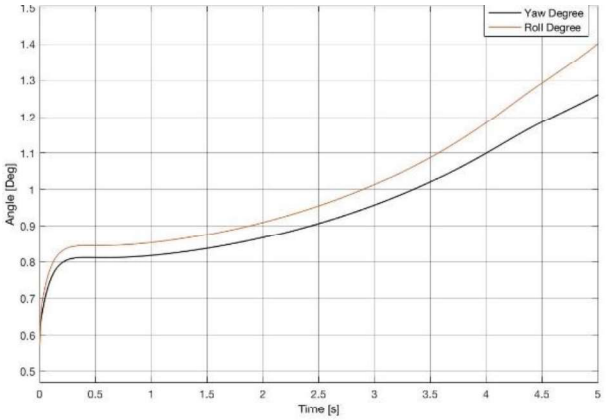

Fig. 5.2 Performance of egress (2).

Then it's time for field test. Before taking from water, the vehicle was under the circumstance that all the water inside the water sump were drained off to make it erect with pitch degree of 80, whose propellers were above water.

With the maximum thrust driving the vehicle out of the water, timestamped photographs of the egress process were recorded and shown in Fig. 7, along with the heights of propeller above water and its vertical velocities shown in Fig. 6.

Stages of egress began with a steady state that its entire body but propellers under water(t=0). Because of the constricted acceleration of thrust, it took about 1s to reach its maximum.

The resultant force is calculated by the equation below.

$$F = T + \rho g v_u - G - f$$

F: Resultant force.

T: Thrust.

G: Gravity of the entire prototype.

ρ: Density of liquid.

v_u: The volume of the vehicle underwater.

f: Total resistance.

Between t=1s and t=1.2s, wings underwater provided considerable amount of v_u which made the resultant F larger than $(T-G)$. In other word, it makes it easier for the vehicle to acquire an initial velocity before its tails leave the surface. Fig.6 shows a velocity of 0.4m/s at the 1.2 seconds as well as an acceleration during that time.

However, with its large wings out of the water, the resistance f increased instantly due to surface tension. Simultaneously, the volume v_u decreased sharply. At this moment, F became smaller than $(T-G)$ which reduce the velocity at 1.3 seconds.

The next stage was predictable between t=1.4s and t=1.9s. The velocity continued to grow before its tail sprung up.

The last stage consisted of analyses of its tail was almost the same as its wings. The difference is that differential tail and horizontal tail can be set to a given angel to adjust the egress angel for the sake of maneuverability. In this field test, the target location was set to the south of the vehicle. The result is shown in Fig.7 (from t=1.9s to t=2.4s).

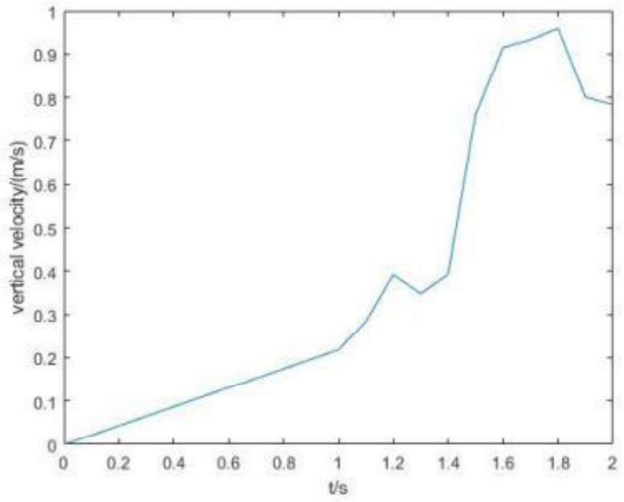

Fig. 6. The corresponding vertical velocity from $t=0$ s to $t=2$ s. Positive direction is ascending.

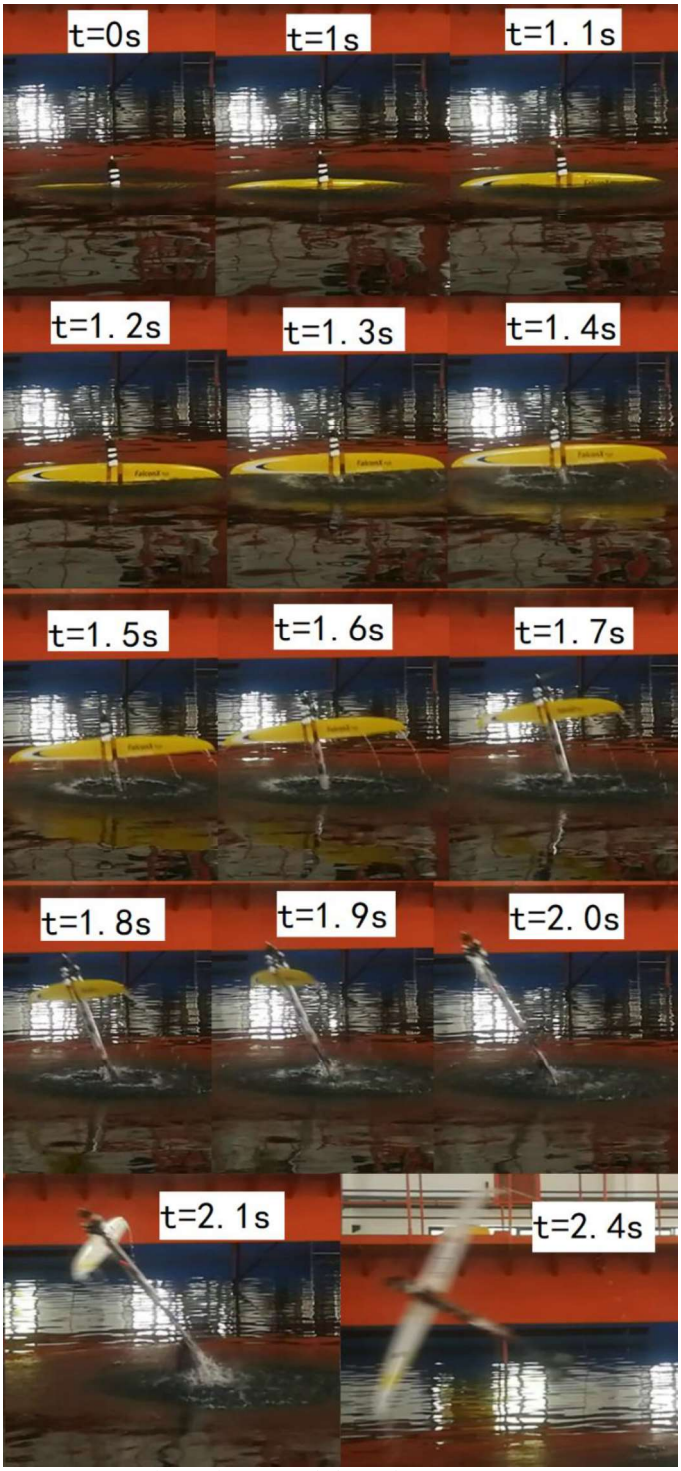

Fig. 7. Timestamped photo of egress.

B. Gliding

The underwater dynamic coefficients of the vehicle were modeled by using DATCOM file. The set depth was about 6 m underwater. In this operation, only the flow rate of the water sump was controlled. For simplification, the environment was supposed to be water uniformly, which differs from the reality.

Due to restriction of the field, gilding with maximum depth over 5 meters could not be performed. Alternatively, similar test was conducted by means of simulation.

Fig. 8 illustrates the relevant data during the gliding operation. The data changes periodically due to the

characteristic of the operation. As we can see, the maximum depth is about 7m. From the graph depth below zero can be observed. This is because of the limitation of the environment settings. The buoyancy does not reduce when the vehicle begins to float at the surface. As in reality this case is impossible to happen, the depth below zero can be simply ignored.

The pitching angles are not large. The maximum magnitude is only about 15 degrees, resulting in the relatively low horizontal velocity. The vertical velocity is small due to the limited change of the overall mass.

The data for the 6-meter test is smooth compared to the results for the field test. This is because the external environment is simplified. The boundary between water and air is ignored, which results in some deviations. More realistic environment models will be built in our future work.

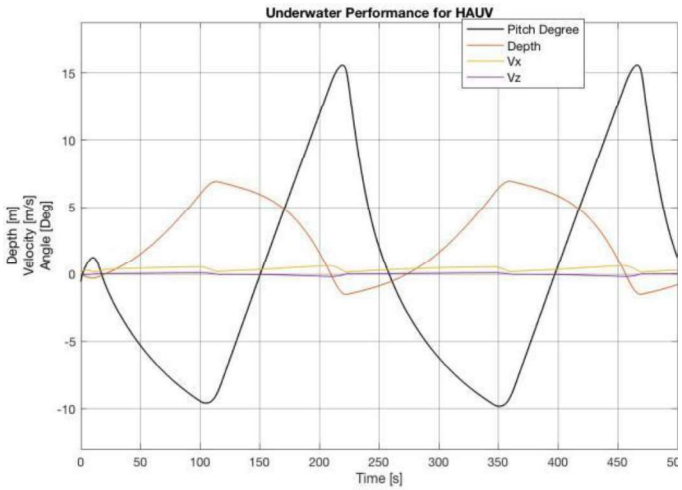

Fig. 8. Performance of 6-meter test.

The field test of gliding was conducted both at Zhiyuan Lake, an artificial lake with the maximum depth of 2 meters in Shanghai Jiao Tong University, and in SJTU UEIC. Target depth can be preset to multiple values via remote control. 0.5-meter test was conduct at Zhiyuan Lake. Time, vertical velocity and depth were recorded (Fig. 9).

The operation began at t=0s, water pump started absorbing until the water sump was full. Once it reached the depth of 0.5m, water would be drained out. But due to the limited flow rate, the vehicle didn't modify its moving direction immediately. It took 10 seconds as long as the time it took to sink to 0.5m to stop descending. It reached the maximum depth of 1.3m and the period of a full cycle is about 56.7s.

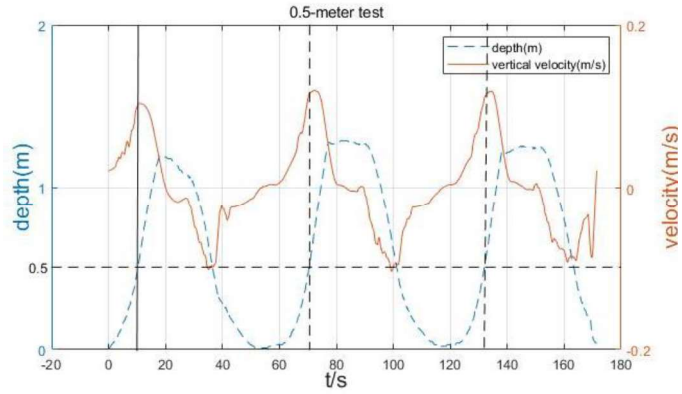

Fig. 9. Performance of 0.5-meter gliding test. The positive direction of vertical velocity is descending.

1-meter test and 2-meter test were conducted in SJTU-UEIC whose data are shown in Fig. 10 and Fig. 11 respectively. The respective maximum depth is 2.9m and3.9m. The respective period is 83.4s and 108.3s. Table 3 shows the overall data of different set-depth.

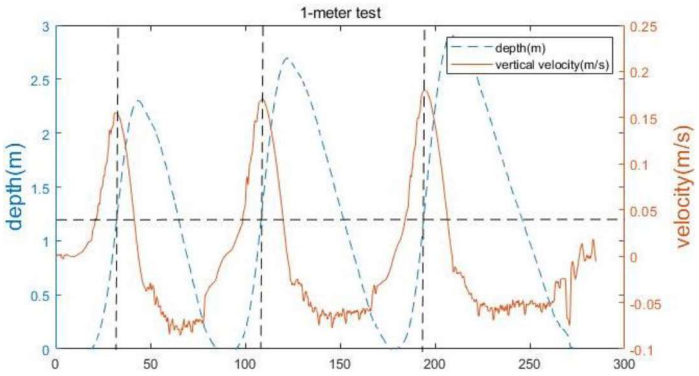

Fig. 10. Performance of 1-meter test.

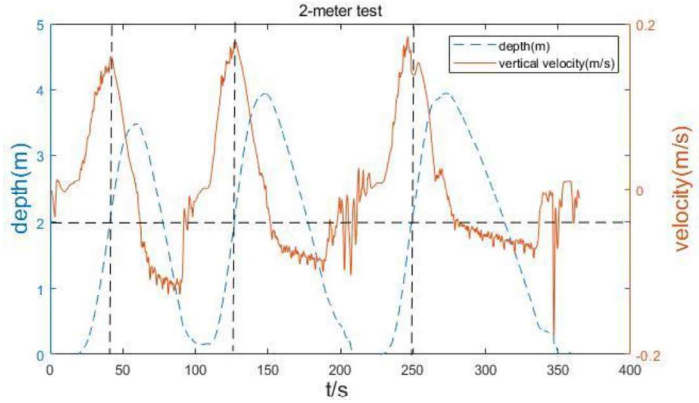

Fig. 11. Performance of 2-meter test.

TABLE III.

SET-DEPTH, MAXIMUM DEPTH AND PERIOD

Set-depth	Max depth	Period
0.5 m	1.3 m	56.7 s
1 m	2.9 m	83.4 s
2 m	3.9 m	108.3 s

C. Discussion

This field testing has confirmed this vehicle's maneuverability of taking off from water and gliding underwater. The largest resistance force occurs when its wings are about to emerge from water. Our test proved that the thrust is large enough to overcome the resistance during the egress. Moreover, its underwater performance is consistent with expected.

Basically, the results of the simulation tests match the data collected during the field tests. The ideal coefficient of the vehicle as well as the simplified environment data make the results smoother than that of the field test. More realistic simulation tests will be conducted in the future work.

V. Conclusion and Future Work

This paper has come up with a new concept of hybrid aerial-aquatic vehicle (HAAV) for large scale and high spatial resolution marine observation. When operating underwater, the aquatic mode of HAAV is featured with its gliding system which enables it to undergo quite a long distance from one water column to another. When meeting with an obstacle, the HAAV egresses from the water and switch to the aerial mode to overpass the obstacle with its propeller. The flexible switch between two modes entitle the HAAV multiple advantages including energy-efficient, easy-to-deploy, multifunctional and highly maneuverable, etc. According to the concept, prototype has been manufactured and verified in field tests. Several experiments and analysis have been conducted and the data are simulated by MATLAB Simulink. The results indicate that the performance of the prototype lives up to the expectation of maneuverability and therefore, this new concept is worth researching.

The future work of improvement will focus on two aspects. One is to improve the capacity of prototype, to increase its thrust, velocity, depth and the robustness of system, to eliminate its weight and cost of energy, etc. The other is to develop new functions, to install camera, Global Positioning System, remote underwater manipulation system, etc. In that case, the applicability as well as the survival rate of prototype in extreme marine conditions can be increased tremendously. Apart from the improvements, the concept of HAAV itself may also inspire other novel concepts in the field of hybrid vehicles in the future, so it is worthwhile to design new prototypes based on the concept and make distinct contributions to large scale and high spatial resolution marine observations.

References

[1] F. Zhang, O. Ennasr, E. Litchman and X. Tan, "Autonomous Sampling of Water Columns Using Gliding Robotic Fish: Algorithms and Harmful-Algae-Sampling Experiments", IEEE Systems Journal, vol. 10, no. 3, pp. 1271-1281, 2016. Available: 10.1109/jsyst.2015.2458173. J. Clerk Maxwell, A Treatise on Electricity and Magnetism, 3rd ed., vol. 2. Oxford: Clarendon, 1892, pp.68–73.

[2] N. E. Leonard, D. A. Paley, R. E. Davis, D. M. Fratantoni, F. Lekien, and F. Zhang, "Coordinated control of an underwater glider fleet in an adaptive ocean sampling field experiment in monterey bay," Journal of Field Robotics, vol. 27, pp. 718-740, 2010.

[3] B. Lyu et al., "Combined Small-sized USV and ROV Observation System for Long-term, Large-scale, Spatially Explicit Aquatic Monitoring", 2019.

[4] Di Lu, Chengke Xiong, Zheng Zeng, and Lian Lian. Adaptive Dynamic Surface Control for a Hybrid Aerial Underwater Vehicle with Parametric Dynamics and Uncertainties. IEEE Journal of Oceanic Engineering, 2019.

[5] R. Siddall, A. Ortega Ancel and M. Kovač, "Wind and water tunnel testing of a morphing aquatic micro air vehicle", Interface Focus, vol. 7, no. 1, p. 20160085, 2016. Available: 10.1098/rsfs.2016.0085.

[6] D. Lu, C. Xiong, B. Lyu, Z. Zeng and L. Lian, "Multi-mode Hybrid Aerial Underwater Vehicle with Extended Endurance", 2019.

[7] H. Alzu'bi, I. Mansour, and O. Rawashdeh, "Loon copter: Implementation of a hybrid unmanned aquatic–aerial quadcopter with active buoyancy control," Journal of Field Robotics, vol. 35, no. 5, pp. 764–778, 2018.

[8] M. M. Maia, D. A. Mercado, and F. J. Diez, "Design and implementation of multirotor aerial-underwater vehicles with experimental results," in 2017 IEEE/RSJ International Conference on Intelligent Robots and Systems (IROS). IEEE, 2017, pp. 961–966.

[9] P. L. Drews, A. A. Neto, and M. F. Campos, "Hybrid unmanned aerial underwater vehicle: Modeling and simulation," in 2014 IEEE/RSJ International Conference on Intelligent Robots and Systems. IEEE, 2014, pp. 4637–4642

[10] D. A. M. Ravell, M. M. Maia, and F. J. Diez, "Modeling and control of unmanned aerial/underwater vehicles using hybrid control," Control Engineering Practice, vol. 76, pp. 112–122, 2018.